THE JOURNAL OF BIOLOGICAL CHEMISTRY

Vol. 268, No. 16, Issue of June 5, pp. 11830-11837, 1993
Printed in U.S.A.

Bidirectional Excision in Methyl-directed Mismatch Repair*

(Received for publication, January 15, 1993)

Michelle Grilley‡, Jack Griffith§, and Paul Modrich¶

From the Department of Biochemistry, Duke University Medical Center, Durham, North Carolina 27710 and the §Lineberger Cancer Research Center and the Departments of Microbiology & Immunology and Biochemistry, University of North Carolina, Chapel Hill, North Carolina 27599-7295

Using electron microscopy and indirect end-labeling methods, we have examined excision tracts produced by the *Escherichia coli* methyl-directed mismatch repair system on a closed circular G-T heteroduplex that contains a single d(GATC) site. Despite differing polarities of the unmodified strand in the two hemimethylated derivatives of the heteroduplex, that portion of the unmethylated strand spanning the shorter path between the d(GATC) site and mismatch is targeted for excision in both cases. Mismatch-provoked excision occurring on both hemimethylated DNAs requires DNA helicase II, but exonuclease requirements for the reaction depend on heteroduplex orientation. When the d(GATC) sequence on the unmodified strand resides 3′ to the mismatch as viewed along the shorter path, excision requires exonuclease I. Excision occurring on the alternate hemimethylated heteroduplex depends on the 5′ → 3′ hydrolytic activity of exonuclease VII. Coupled with the previous demonstration that repair initiates via the mismatch-provoked, MutHLS-dependent incision of the unmethylated strand at a d(GATC) sequence (Au, K. G., Welsh, K., and Modrich, P. (1992) *J. Biol. Chem.* 267, 12142–12148), these findings indicate an excision mechanism in which helicase II displacement renders the incised strand sensitive to the appropriate single-strand exonuclease. Our data imply that hydrolysis commences at the d(GATC) site, proceeds to a point beyond the mismatch, and terminates at a number of discrete sites within a 100-nucleotide region just beyond this site. The extent of excision is therefore controlled by one or more components of the repair system.

In *Escherichia coli*, methyl-directed mismatch repair eliminates biosynthetic errors from newly replicated DNA in a reaction dependent on 10 activities (1, 2), with the requisite strand specificity provided by the transient undermethylation of d(GATC) sequences in the newly synthesized strand. Repair is initiated by the mismatch-provoked incision of the unmethylated strand at a hemimethylated d(GATC) site, a reaction dependent on MutH, MutL, MutS, and ATP (3). The resulting strand break suffices to target repair to the unmodified DNA strand (1, 4). A striking feature of the methyl-directed reaction is that it is independent of heteroduplex orientation: a single d(GATC) sequence located either 3′ or 5′ to the mismatch on the unmethylated strand is sufficient to direct repair (2, 3).

Although correction of both heteroduplex orientations requires MutH, MutL, MutS, DNA helicase II, single-strand DNA binding protein (SSB),[1] DNA polymerase III holoenzyme, and DNA ligase (Ref. 1 and below), the exonuclease requirements of the reaction are orientation-specific. When directed by a d(GATC) sequence located 3′ to the mismatch on the unmodified strand, repair requires exonuclease I (2), an activity that hydrolyzes single-stranded DNA with 3′ → 5′ polarity (5). Conversely, repair directed by a d(GATC) sequence 5′ to the mismatch depends on either exonuclease VII or RecJ exonuclease, both of which catalyze 5′ → 3′ hydrolysis of single strands (6, 7). These observations have led to the suggestion that the methyl-directed system is capable of bidirectional excision (2), a view that is confirmed in this paper by direct analysis of mismatch-provoked excision tracts. We also describe contributions of individual repair proteins to the excision process. An accompanying manuscript (8) demonstrates that strand-specific mismatch correction in nuclear extracts of human cells shares a similar bidirectional excision capability.

EXPERIMENTAL PROCEDURES

Materials—*E. coli* and phage strains used in this work are described in the accompanying paper (2). Hemimethylated supercoiled f1 G-T heteroduplex DNA and a control G·C homoduplex (Fig. 1) were prepared as described previously (9, 10). For reasons summarized in Fig. 1, we refer to molecules bearing d(GATC) modification on the complementary or viral strand as 3′- or 5′-substrates, respectively. The f1MR3 RF DNA (10) used to generate sequence ladders and as molecular weight markers for gel electrophoresis was prepared by standard methods (11) and contained an unmethylated d(GATC) sequence.

*Eco*47III endonuclease and avian myeloblastosis virus reverse transcriptase were from U. S. Biochemical Corp., *Bsp*106 endonuclease was from Stratagene, other restriction enzymes were purchased from New England Biolabs, and streptavidin was from Sigma. With the exception of biotin-11-dCTP, which was from ENZO Biochemicals, nucleotides were purchased from Pharmacia LKB Biotechnology Inc. Sources of other proteins are specified in the accompanying manuscript (2).

Mismatch Repair Reactions—Methyl-directed mismatch repair in *E. coli* cell-free extracts was performed as described previously (12) except that reactions were supplemented with 0.08 M KCl, and when indicated, the four 2′,3′-dideoxynucleoside-5′-triphosphates (ddNTPs, 0.1 mM each) were substituted for 2′-deoxynucleoside-5′-triphosphates (dNTPs). Incubation was at 37 °C for 30 min. Repair in a purified system (1, 2) was assayed in reactions containing 0.05 M HEPES-KOH, pH 8.0, 0.02 M KCl, 6 mM $MgCl_2$, 1 mM dithiothreitol, 0.05 mg/ml bovine serum albumin, 2 mM ATP, 0.1 mM each dATP, dCTP, dGTP, and dTTP (or, when indicated, 0.1 mM each ddATP,

* This work was supported by Grants GM23719 (to P. M.) and GM31819 (to J. G.) from the National Institute of General Medical Sciences. The costs of publication of this article were defrayed in part by the payment of page charges. This article must therefore be hereby marked "*advertisement*" in accordance with 18 U.S.C. Section 1734 solely to indicate this fact.

‡ Present address: Dept. of Biology, University of Utah, Salt Lake City, UT 84112.

¶ To whom correspondence and reprint requests should be addressed. Tel.: 919-684-2775; Fax: 919-684-8885.

[1] The abbreviations used are: SSB, single-strand DNA binding protein; kb, kilobase(s); bp, base pair(s).

ddCTP, ddGTP, and ddTTP), 25 μM NAD^+, 10 μg/ml DNA, 26 ng/ml MutH, 1.7 μg/ml MutL, 3.5 μg/ml MutS, 20 μg/ml SSB, 1 μg/ml DNA helicase II, 0.1 μg/ml exonuclease I, 6 μg/ml exonuclease VII, 2 μg/ml *E. coli* DNA ligase, and 9.5 μg/ml DNA polymerase III holoenzyme. Holoenzyme was purified according to McHenry and Kornberg (13) and was free of significant 5′ to 3′ exonuclease activity (2). Incubation was at 37 °C for 20 min.

Electron Microscopy—Repair reactions were terminated by addition of EDTA to 15 mM, and DNA was purified by phenol extraction and passage through a 4-ml Sephadex G-50 column equilibrated in 0.01 M Tris-HCl, pH 7.6, 1 mM EDTA, followed by ethanol precipitation. DNA was linearized at the unique *Cla*I site at position 2529 (Fig. 1), and the resulting termini were filled in with biotin-11-dCTP and dGTP in a reaction containing 0.05 M Tris-HCl, pH 8.0, 5 mM $MgCl_2$, 0.05 M KCl, 5 mM dithiothreitol, 0.05 mg/ml bovine serum albumin, 29 μg/ml DNA, 0.02 mM biotin-11-dCTP, 0.02 mM dGTP, and 500 units/ml avian myeloblastosis virus reverse transcriptase. After 45 min at 37 °C, labeling was terminated by heating to 60 °C for 10 min. Samples were then supplemented with an equal volume of 0.01 M Tris-HCl, pH 7.5, 0.1 M NaCl, 0.01 M $MgCl_2$, and 1 mM dithiothreitol, and the DNA was cleaved into 5.9-kilobase and 0.5-kilobase fragments by treatment with *Eco*47III endonuclease (Fig. 1). (A second *Eco*47III recognition sequence is present within the 0.5-kb fragment, but hydrolysis at this site was not observed under the conditions used.) After phenol extraction and ethanol precipitation, DNA (15 μg/ml) was incubated in 0.05 M HEPES-KOH, pH 8.0, 6 mM $MgCl_2$, 0.02 M KCl, 1 mM dithiothreitol, 0.02 mg/ml SSB, and 0.036 mg/ml streptavidin for 10 min at room temperature. Protein-DNA complexes were fixed and prepared for viewing as described previously (14). Micrographs were taken using a Phillips EM400 TLG electron microscope. Positions of the SSB-coated DNA segments were measured relative to the streptavidin-labeled and unlabeled termini using a Summagraphics digitizer coupled to an IBM PC/AT computer. Lengths of wholly duplex molecules were used as a standard to convert digitizer output into base pairs. Measurements of the duplex 5.9-kb *Eco*47III-*Cla*I fragment had a precision of ±350 bp (± 2 S.D.). Since the distance from an end to the nearest double-strand/single-strand junction was about 2.4 kb, we estimate the error in locating gap end points by microscopy to be ±150 bp, ignoring any difficulties in precise assignment of this junction.

Analysis of Gaps by Indirect End-labeling—Repair reactions were terminated by addition of EDTA to 15 mM, and the DNA was purified by phenol extraction and ethanol precipitation. DNA was then either hydrolyzed with *Cla*I (or its isoschizomer *Bsp*106) or *Eco*47III endonuclease and separated on 1.1% alkaline agarose gels (11) or, alternatively, hydrolyzed with *Hga*I, *Ssp*I, or *Xmn*I endonuclease, extracted with phenol, ethanol-precipitated, resuspended in 80% formamide, 0.01 M NaOH, 1 mM EDTA, 0.025% bromphenol blue, and 0.025% xylene cyanol and loaded on 40-cm 5% polyacrylamide sequencing gels along with the appropriate sequence ladders. Sequence ladders were prepared from f1MR3 RF DNA (10) by the dideoxy termination method using Sequenase Version 2.0 (United States Biochemical Corp.) or by Maxam-Gilbert chemical cleavage (15). DNA bands were visualized by hybridization with 5′-^{32}P-oligonucleotide probes (Table I) at 37 °C as described previously (3) after electrotransfer to nylon membranes (16).

RESULTS

Excision Tracts Generated in Cell-free Extracts as Visualized by Electron Microscopy—Using a hemimethylated 3′-circular G-T heteroduplex (Fig. 1), we have previously shown that excision and resynthesis steps of methyl-directed repair in *E. coli* extracts can be resolved when DNA synthesis is inhibited by ddNTPs (14). Electron microscopic visualization of DNA products produced under these conditions revealed the presence of single-strand gaps that spanned the shorter path between the mismatch and the d(GATC) site in the circular substrate (14). Since gap formation was dependent on functional *mutH* and *mutS* gene products as well as DNA synthesis inhibition, these structures were attributed to a mismatch-provoked excision reaction. The results of this earlier study (14) are summarized in Fig. 2*A* to permit their comparison with new findings described here.

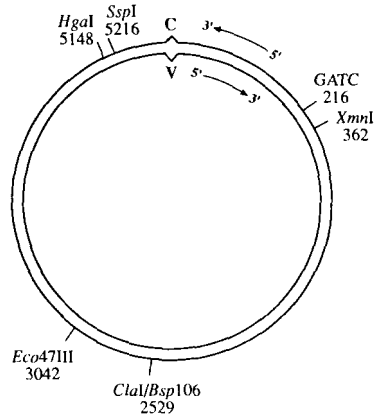

FIG. 1. **Heteroduplex DNAs.** The 6440-base pair covalently closed circular heteroduplex used in this work contained a G-T mismatch at coordinate 5632 and a single d(GATC) sequence at position 216, which was modified on the viral (*V*) or complementary (*C*) DNA strand (10, 20). Since hemimethylation imposes an asymmetry on the helix, heteroduplexes are designated according to orientation of the unmodified strand. Molecules bearing complementary strand methylation are referred to as 3′-heteroduplexes since the unmodified d(GATC) sequence that directs repair is located 3′ to the mismatch along the shorter path (1024 bp) separating the two sites in the circular molecule. The substrate with viral strand modification is designated a 5′-heteroduplex for a similar reason. Cleavage sites of restriction enzymes used in the analysis of excision intermediates are shown. *Hga*I, *Ssp*I, and *Xmn*I each cleave at multiple sites, but only the sites relevant to this study are shown. A second *Eco*47III recognition sequence is present at position 2713, but cleavage at this site was not observed under the conditions used.

We have extended this analysis to excision intermediates produced in cell-free extracts with the corresponding 5′-circular G-T heteroduplex (Fig. 2*D*). Fifty percent of the product molecules examined in the electron microscope contained single-strand regions (a minimum of 150 molecules were counted in each case), and these gaps resulted from provocation of mismatch correction as judged by several criteria. The fraction of molecules undergoing mismatch repair in the presence of exogenous dNTPs (47%) corresponded well with the fraction of gapped molecules observed in reactions inhibited by ddNTPs (50%). Furthermore, the yield of molecules containing a single-strand gap was reduced substantially when dNTPs were substituted for ddNTPs (6%), when the extract was derived from an isogenic *mutS*$^-$ strain (10%) or when 5′-G·C homoduplex DNA was substituted for heteroduplex DNA in a *mut*$^+$ extract (9%).

The orientation of the unmodified strand in this 5′-heteroduplex is reversed relative to that in the 3′-heteroduplex examined previously (14), but the location and distribution of single-strand regions were similar for the two DNAs (Fig. 2, *D* and *A*). The average length of excision tracts observed with the 5′-substrate was 1500 ± 800 (± 1 S.D.) nucleotides, similar to the 1500 ± 480 nucleotide gap size determined previously

TABLE I

Oligonucleotide probes used in this study

Oligonucleotides were synthesized and 5′-end-labeled as described previously (3). Oligonucleotides are designated by strand and location of the sequence within the f1MR3 duplex (10). The coordinate specifies the location of the underlined nucleotide.

Oligonucleotide	Sequence
V2531	d(ATGGTTTCATTGGTGACGTT)
C2667	d(CCGATTGAGGGAGGGAAGGT)
V362	d(TAAAACGCGATATTTGAAGT)
C362	d(ACTTCAAATATCGCGTTTTA)
V5216	d(ATTGTTCTGGATATTACCAG)
C5148	d(TTGACGCTCAATCGTCT)

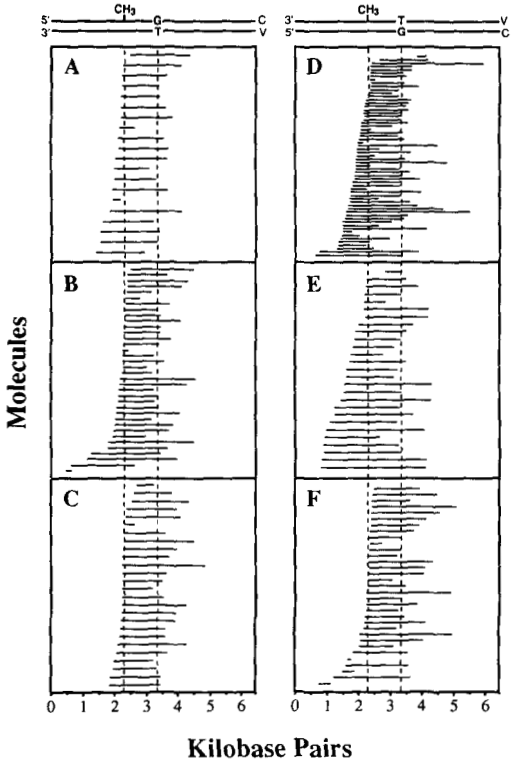

FIG. 2. **Mapping of excision tracts by electron microscopy.** 3′-Circular (*panels A-C*) and 5′-circular (*panels D-F*) G-T heteroduplex DNAs were incubated in the presence of ddNTPs with cell-free extract prepared from repair-proficient *E. coli* or with the purified repair system (see "Experimental Procedures"). *Panels B-F*, after termination of repair reactions, DNA products were prepared for electron microscopy, and single-strand gaps were mapped as described under "Experimental Procedures." Each *horizontal line* represents a single-strand region within an individual molecule. The estimated error in assignment of gap end points is ±150 bp (see "Experimental Procedures"). *Panel A*, data from a previous study (14) are included here for comparison. *Gaps* are presented relative to the *Cla*I restriction site used for mapping of the molecules shown in *Panels B-F*. *Panels A* and *D*, cell-free extract derived from *E. coli* AB1157. *Panels B* and *E*, purified mismatch repair system. *Panels C* and *F*, purified system lacking the exonuclease that is not required for repair of the particular hemimethylated DNA (exonuclease VII or exonuclease I omitted for *Panels C* and *F*, respectively).

for the 3′-heteroduplex (14). In the majority of the molecules examined (41/61), excision tracts span both the d(GATC) site and the mismatch and were localized to the shorter path separating the two sites in the circular DNA.[2] Another major class of products (14 of 61 molecules) may be due to aborted repair events. These molecules contained either very small single-strand regions located near the d(GATC) site or larger gaps that extended from the d(GATC) site toward the mismatch via the longer path separating the two sites in the circular DNA (Fig. 2*D, bottom*). The latter structures may reflect infrequent, aborted attempts to excise via the longer path joining the d(GATC) site and the mismatch, but they could also have been produced by adventitious exposure of incised or gapped molecules to nucleases in the extract.

Since gapped circular molecules were examined by microscopy after treatment with *Cla*I and *Eco*47III (Fig. 1, see "Experimental Procedures"), circles with single-strand regions spanning the *Cla*I-*Eco*47III region are expected to be resistant to these activities. The possible occurrence of excision tracts spanning this region was excluded by the finding that less than 2% of the molecules observed by microscopy were circles that were partially or wholly single-stranded. Thus, despite identification of the few molecules mentioned above that may represent attempts to excise via the longer path separating the d(GATC) site and mismatch in the circular heteroduplex, it is clear that effective excision is restricted to the shorter path joining the two sites. These findings, coupled with our previous observations with the 3′-heteroduplex (Fig. 2*A* and Ref. 14), indicate that the methyl-directed excision reaction is independent of d(GATC) → mismatch orientation, but rather is governed by proximity of the two sites along the helix contour. The finding that distinct exonucleases with different hydrolytic polarities are required for repair of the two hemimethylated forms of this circular heteroduplex (2) is also consistent with this view.

Excision Tracts Generated in a Purified Repair System—Using electron microscopy, we have also examined excision intermediates produced in a purified mismatch repair system comprised of MutS, MutL, MutH, DNA helicase II, SSB, DNA polymerase III holoenzyme, DNA ligase, exonuclease I, and exonuclease VII. The accompanying paper (2) demonstrates that either exonuclease VII or RecJ is necessary for 5′-heteroduplex repair. We have used exonuclease VII in the experiments described here. This set of nine activities supports methyl-directed repair of heteroduplex DNA and displays a mismatch specificity similar to that observed *in vivo* and in cell-free extracts (1, 2). Incubation of 3′- or 5′-circular G-T heteroduplexes with these components in the presence of ddNTPs also produced single-strand gapped intermediates. As shown in Table II, formation of these intermediates with 3′- or 5′-circular heteroduplexes was dependent on the presence of a mismatch, MutS, and MutL, and the yield of gapped molecules produced in the presence of ddNTPs correlated extremely well with the extent of mismatch repair in parallel reactions containing dNTPs.

Virtually identical products were obtained with the 3′-heteroduplex in the two systems (Fig. 2, *A* and *B*). The average length of single-strand regions produced in the purified system (1,400 ± 630 nucleotides) was indistinguishable from that of

TABLE II

Requirements for gap formation in the purified system

Hemimethylated G-T heteroduplex or hemimethylated control homoduplex DNA was treated with the purified repair system in the presence of dNTPs or ddNTPs as described under "Experimental Procedures." Products produced in the presence of dNTPs were tested for repair, while those produced in the presence of ddNTPs were examined by electron microscopy for single-strand gaps, which were scored as regions labeled by SSB (see "Experimental Procedures"). Results are based on examination of at least 150 molecules for each sample. The low but significant level of activity observed with G·C control homoduplexes is due to damage incurred during strand separation and annealing steps involved in substrate preparation or to natural variation in DNA samples used for this purpose (3).

Substrate orientation	G-T mismatch	Components omitted	SSB-labeled molecules	Mismatch repair
			%	
5′	+	Complete	57	47
5′	+	−Exonuclease I	58	55
5′	+	−MutL	2	<5
5′	G·C	Complete	10	
3′		Complete	72	67
3′	+	−Exonuclease VII	71	69
3′	+	−MutS	3	<5
3′	G·C	Complete	8	

[2] A gap with one end between the d(GATC) site and the mismatch was scored as spanning the two sites if that end was located within 150 nucleotides of the closer site. As described under "Experimental Procedures," single-strand/double-strand junctions were located by measurement of duplex segment length, a procedure with an estimated error of ±150 bp.

the extract reaction (1,500 ± 480 nucleotides), and in both cases about 80% of the single-strand regions spanned the shorter distance between the d(GATC) site and the mismatch (28/36 and 15/20 molecules).[2] Omission of exonuclease VII, which is not required for repair of this heteroduplex orientation (2), had little effect on the size (1,500 ± 480 nucleotides) or location of excision tracts which spanned the two sites in 22 of the 26 molecules measured (Fig. 2, *B* and *C*).

While excision tracts produced on the 5′-heteroduplex in the purified repair system were generally similar to those generated in cell-free extracts, several differences between the products of the two systems were apparent (Fig. 2, *D* and *E*). As in the case of the extract reaction, the majority of the excision tracts produced in the purified system spanned the d(GATC) site and the mismatch (21 of 27 molecules). However, molecules containing short gaps near the d(GATC) site, which represented about 10% of the extract product, were not observed among products of the reconstituted reaction. Excision tracts produced in the purified system (2,000 ± 780 nucleotides) were larger than those observed with this substrate after incubation with *E. coli* extracts (1,500 ± 800 nucleotides). This difference is largely attributable to the absence of small gaps in products of the purified system and to a small extent reflects an increased frequency in the number of molecules containing larger gaps that extend to the 5′-side of the d(GATC) sequence on the unmodified strand (Fig. 2*E*). Omission of exonuclease I, which is not required for 5′-heteroduplex repair (2), did not alter the frequency of excision tracts that spanned the d(GATC) sequence and the mismatch, with gaps spanning the two DNA sites in 26 of 33 molecules examined (Fig. 2*F*). Single-strand regions observed in this case had an average size of 1,500 ± 710 nucleotides and were characterized by relatively precise localization of the end near the d(GATC) site.

Mapping of Excision Tract End Points by Indirect End-labeling—Due to the limited number of molecules that can be examined by electron microscopy, we have used an indirect end-labeling method to confirm the location of excision tract end points generated in the purified system. In this procedure, excision tract end points within the circular substrate were mapped relative to restriction endonuclease cleavage sites after electrophoretic separation under denaturing conditions (see "Experimental Procedures"). The results of such an analysis with the 5′-G-T heteroduplex in the purified system are presented in Fig. 3. In the absence of MutS, or when 5′-G·C homoduplex was substituted for heteroduplex DNA, the unmodified strand was recovered as a full length 6.4-kb species (*lanes 1, 2, 9,* and *10*). In contrast, incubation of the 5′-heteroduplex with the complete repair system produced discontinuities in the unmethylated complementary strand with end points near the mismatch and d(GATC) sequence (*lanes 4* and *12*), and the locations of these end points were largely unaffected by omission of exonuclease I (*lanes 3* and *11*), which is not necessary for correction of this substrate (2). Under both reaction conditions, a major end point was observed about 100 nucleotides 3′ to the mismatch, with some hydrolysis proceeding beyond this position in both cases. In the absence of exonuclease I, a major terminus was observed very near the location of the d(GATC) sequence, with a second minor end point evident about 300 nucleotides 5′ to this site. These termini were also the major species observed in the presence of exonuclease I, but in this case the intensity of bands in this region was diminished, and distribution of termini between the two sites was approximately equivalent. This suggests that 3′ → 5′ hydrolysis from the d(GATC) sequence by exonuclease I confers additional variability on

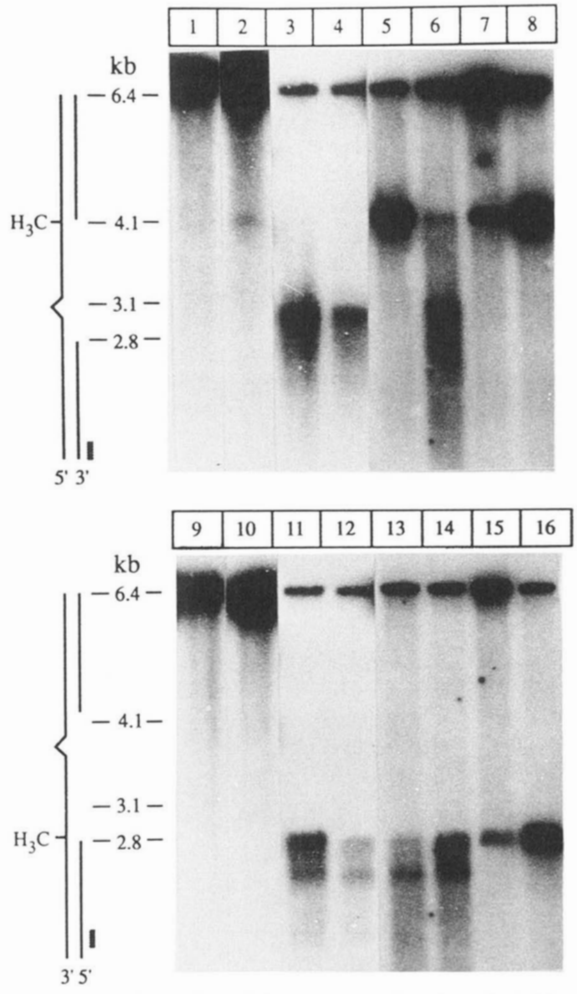

FIG. 3. **Mapping of excision tract end points in 5′-heteroduplexes by indirect end-labeling.** 5′-G-T heteroduplex and 5′-G·C homoduplex substrates were incubated with the purified repair system in the presence of ddNTPs as described under "Experimental Procedures," with repair components omitted as indicated. Products were hydrolyzed with *Cla*I endonuclease (*lanes 1–8*) or *Eco*47III endonuclease (*lanes 9–16*), separated by electrophoresis through alkaline agarose, and electrotransferred to nylon membranes (see "Experimental Procedures"). Membranes were probed with radiolabeled oligonucleotide V2531 (Table I) which hybridizes to the complementary strand within the 500-nucleotide region between the *Cla*I and *Eco*47III sites. The anticipated structure of the product of the complete reaction, based on microscopy data, is illustrated at the *left* of the figure, with the *vertical bar* indicating the location of the V2531 sequence. *Lanes 1* and *9*, heteroduplex; MutS omitted. *Lanes 2* and *10*, G·C homoduplex DNA; complete repair system. *Lanes 3* and *11*, heteroduplex; exonuclease I omitted. *Lanes 4* and *12*, heteroduplex; complete repair system. *Lanes 5* and *13*, heteroduplex; exonuclease VII omitted. *Lanes 6* and *14*, heteroduplex; exonuclease I and DNA polymerase III holoenzyme omitted. *Lanes 7* and *15*, heteroduplex; exonuclease I, DNA polymerase III holoenzyme, and DNA helicase II omitted. *Lanes 8* and *16*, heteroduplex; exonuclease I, DNA polymerase III holoenzyme, DNA helicase II, and DNA ligase omitted.

generation of the termini 5′ to this site. The results of these end-labeling experiments with the two hemimethylated heteroduplexes are therefore consistent with the electron microscopic findings, but they suggest that excision tract end points are somewhat more discrete than implied by microscopy.

We have also used the indirect end-labeling procedure to evaluate contributions of required proteins to the excision reaction. Exonuclease VII is required for repair of the 5′-heteroduplex (2), and its omission from the purified system blocked excision on this substrate. A discontinuity was intro-

duced into the unmodified strand under these conditions, but both 3′- and 5′-termini mapped near the d(GATC) site (Fig. 3, *lanes 5* and *13*). Given that methyl-directed repair initiates by the mismatch-provoked, MutHLS-dependent incision of the unmodified strand at a d(GATC) site (3), this observation demonstrates that exonuclease VII functions in the reaction as a 5′ → 3′ hydrolytic activity that initiates attack at the incised d(GATC) sequence.

As might be expected from the finding that excision and resynthesis steps in repair can be resolved by blocking DNA synthesis, DNA polymerase III holoenzyme is not required for the excision stage of the reaction. Termini produced in the absence of holoenzyme and exonuclease I (Fig. 3, *lanes 6* and *14*) were similar to those observed when only exonuclease I was omitted from the reaction (*lanes 3* and *11*), although some hydrolysis into the region 5′ to the d(GATC) site was observed in the absence of holoenzyme suggesting that action of the DNA polymerase stabilizes 3′-termini in this region. However, omission of holoenzyme, exonuclease I, and DNA helicase II resulted in an excision block. The 3′- and 5′-termini produced under these conditions were located at the d(GATC) sequence (*lanes 7* and *15*), and the yield of product molecules with a discontinuity at this position increased substantially when DNA ligase was also omitted from the reaction (*lanes 8* and *16*). Helicase II and exonuclease VII are therefore both required for the excision step in correction of a 5′-heteroduplex. These observations also imply that the excision system and ligase compete for the single-strand break that is introduced at the d(GATC) during the initiation of repair, a conclusion consistent with prior observations indicating that a pre-existing single-strand break can effectively direct mismatch repair only in the absence of DNA ligase (1, 4).

Similar results were obtained with the 3′-circular heteroduplex except that the roles of exonuclease VII and exonuclease I were reversed (Fig. 4). Products derived from this substrate contained major discontinuities within the unmodified strand that were located near the d(GATC) site and about 100 nucleotides 5′ to the mismatch (*lanes 4* and *12*). Formation of these termini required MutS (*lanes 1* and *9*) and a mismatch (*lanes 2* and *10*), but was independent of the presence of exonuclease VII (*lanes 3* and *11*) and DNA polymerase III holoenzyme (*lanes 6* and *14*). However, excision was dependent on exonuclease I (*lanes 5* and *13*). In the absence of this activity, major 5′-end points occurred near the d(GATC) sequence, and 3′-termini were broadly distributed over a 700-nucleotide region extending from the d(GATC) site toward the mismatch (*lanes 5* and *13*). We attribute production of the latter products to exonucleolytic hydrolysis commencing from the d(GATC) site by 3′ → 5′ activity of exonuclease VII. Despite the high relative concentration of exonuclease VII used in these experiments (35 mol of exonuclease VII per mol of exonuclease I), it is clear that the 3′ → 5′ activity of this enzyme is much less effective than exonuclease I in promoting excision on the 3′-heteroduplex, in accord with the previous finding that exonuclease VII will not substitute for exonuclease I in repair of this substrate (2). In addition to the exonuclease I requirement, excision on the 3′-heteroduplex was absolutely dependent on DNA helicase II. As observed with the 5′-heteroduplex, processing of the unmodified strand in the absence of this activity was a limited to incision at the d(GATC) site to produce a ligase-sensitive single-strand break (*lanes 7, 8, 15,* and *16*).

Fine Structure Mapping of Excision Tract End Points—The procedure used here to trap excision intermediates has the drawback that gapped molecules accumulating in the reaction may be subject to adventitious exonuclease attack, which would confer additional variability on the actual end point distribution. Indeed, while significant variability was apparent in the location of individual end points determined by the methods described above, these experiments also indicated occurrence of fairly discrete termini near the mismatch and the d(GATC) site in major subpopulations of product molecules. Since the latter end points may represent the primary products of excision, we have used sequencing gels to map their locations at the nucleotide level. Fig. 5 shows the distribution of end points, which were generated in the purified system, in a 250-nucleotide region spanning the mismatch. For both 5′- and 3′-heteroduplexes, the majority of the termini occurred within a 100-nucleotide region just beyond the mismatch. Furthermore, the distribution of end points was

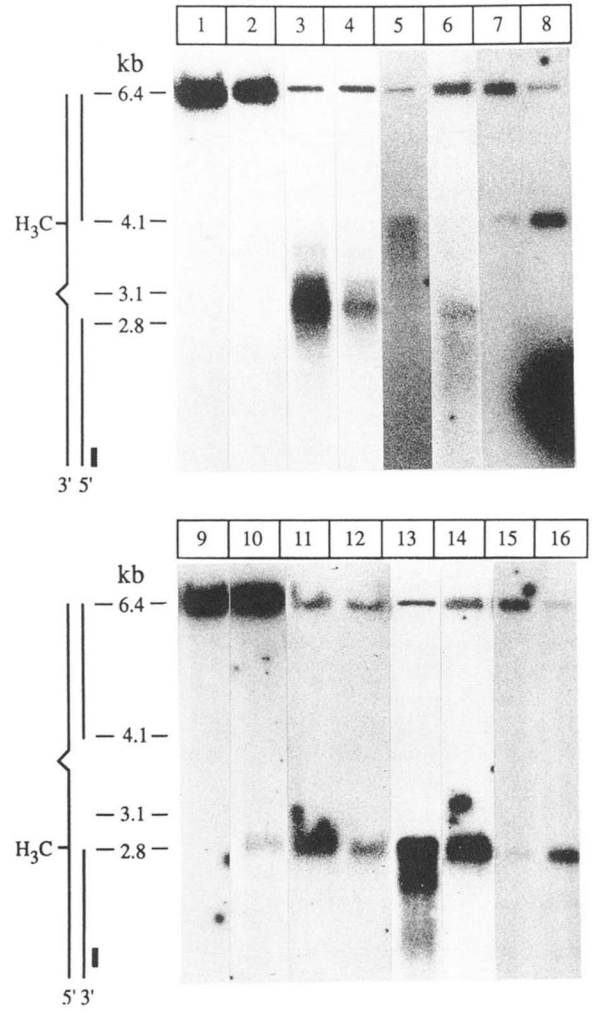

FIG. 4. **Mapping of excision tract end points in 3′-heteroduplexes by indirect end-labeling.** Samples were prepared and analyzed as described in the legend to Fig. 3, except that substrates were 3′-circular G-T or G·C DNAs, and membranes were probed oligonucleotide C2667, which is complementary to the unmethylated strand (Table I). Although not shown, probing of membranes with an oligonucleotide that hybridized to the modified strand demonstrated that this DNA strand remained intact under all conditions. *Lanes 1* and *9*, heteroduplex; MutS omitted. *Lanes 2* and *10*, homoduplex DNA; complete repair system. *Lanes 3* and *11*, heteroduplex; exonuclease VII omitted. *Lanes 4* and *12*, heteroduplex; complete repair system. *Lanes 5* and *13*, heteroduplex; exonuclease I omitted. *Lanes 6* and *14*, heteroduplex; exonuclease VII and DNA polymerase III holoenzyme omitted. *Lanes 7* and *15*, heteroduplex; exonuclease VII, DNA polymerase III holoenzyme, and DNA helicase II omitted. *Lanes 8* and *16*, heteroduplex; exonuclease VII, DNA polymerase III holoenzyme, DNA helicase II, and DNA ligase omitted.

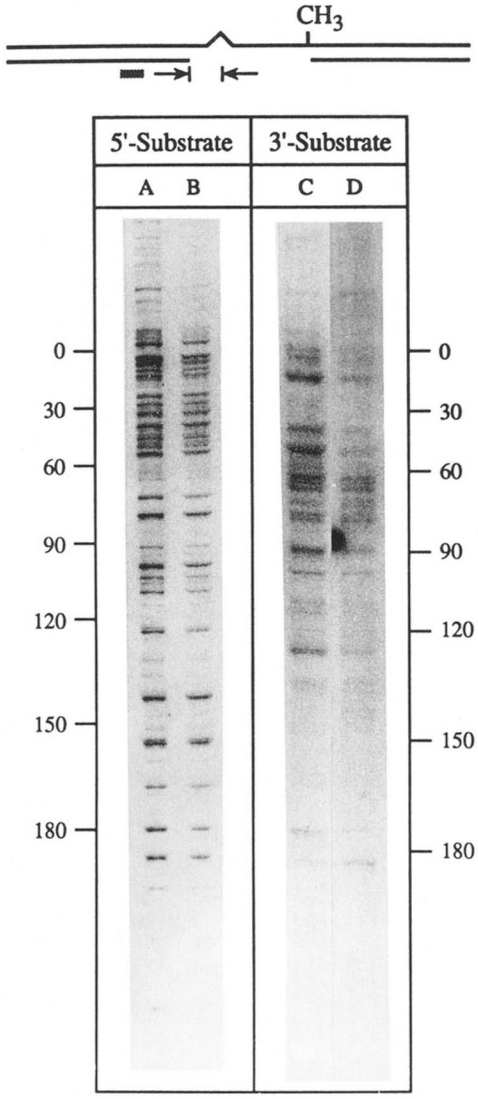

FIG. 5. **Fine structure mapping of excision tract end points near the mismatch.** Repair reactions with the purified system were performed in the presence of ddNTPs as described under "Experimental Procedures" using 5′- or 3′-circular G-T heteroduplexes. DNA products were hydrolyzed with either *Ssp*I (5′-substrate) or *Hga*I (3′-substrate), separated on 5% sequencing gels, transferred to nylon membranes, and probed with radiolabeled oligonucleotides (*hatched bar*) V5216 for the 5′-heteroduplex or C5148 for the 3′-heteroduplex (Table I). Termini mapped in these experiments are expected to be 5′-phosphoryls for the 5′-substrate and dideoxy-terminated 3′-ends for the 3′-substrate. Nucleotide positions on the *ordinate* are relative to the mismatch (position 0) and were determined by parallel electrophoresis of sequencing ladders generated by the dideoxy method (markers for 3′-heteroduplex) or the chemical method (markers for 5′-heteroduplex). *Lanes B* and *D*, complete repair system. *Lane A*, exonuclease I omitted. *Lane C*, exonuclease VII omitted.

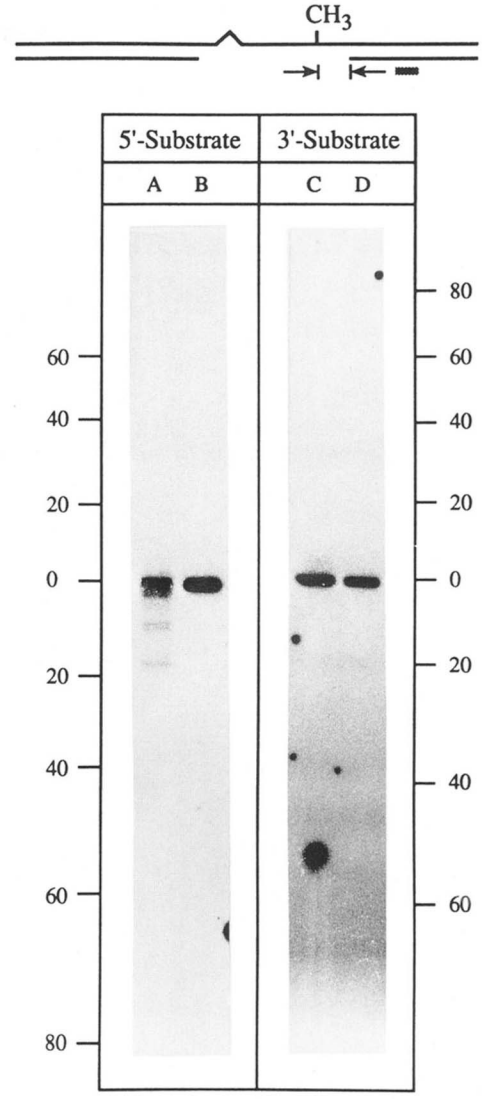

FIG. 6. **Fine structure mapping of excision tract end points near the d(GATC) sequence.** Repair reactions and electrophoretic analysis were performed as described in the legend to Fig. 5 except that the exonuclease not required for repair of the particular heteroduplex was omitted from the reactions and DNA products were hydrolyzed with *Xmn*I prior to electrophoresis. Gel transfers were visualized by hybridization with oligonucleotide V362 (Table I) for the 5′-heteroduplex and C362 for the 3′-substrate. Nucleotide positions on the *ordinate* are relative to the the d(GATC) site (position 0) and were determined by parallel electrophoresis of sequencing ladders. *Lanes A* and *C*, repair reaction products. *Lanes B* and *D*, homoduplex f1MR3 RF DNA cleaved with *Xmn*I and *Mbo*I. *Mbo*I cleaves at d(GATC) sites with the same positional specificity as the activated form of MutH (3).

non-random within this region for both DNAs, and in each case was independent of the presence of the exonuclease that is not required for repair of the particular heteroduplex orientation (compare *lanes A* and *B* and *lanes C* and *D*).

We have also examined the fine structure of end points in the vicinity of the d(GATC) sequence. Since the agarose gel experiments described above indicated a bimodal distribution of end points near this site when both exonucleases were included in the reconstituted system (Fig. 3), these experiments were performed in the presence of only the particular exonuclease that is required for repair of the heteroduplex being examined. As shown in Fig. 6 (*lanes C* and *D*), the only detectable terminus produced under these conditions within a 140-nucleotide region spanning the d(GATC) site was located at the site of cleavage by the activated form of MutH (ϕpGpApTpC) (3). Very similar results were obtained with the 5′-heteroduplex (*lanes A* and *B*), except that in this case several minor termini were evident within the 20-nucleotide region 3′ to the d(GATC) sequence. Comparison of these results with those shown in Figs. 3 and 4 (*lane 11*) demonstrates that in a major fraction of product molecules, the gap end point near the d(GATC) sequence corresponds to the location of the cleavage event that occurred during the initiation step of repair.

DISCUSSION

A major conclusion of this work is that the methyl-directed mismatch repair system possesses a bidirectional excision capability. This finding is consistent with the previous observation that mismatch-provoked d(GATC) incision by the activated form of MutH can occur either 3′ or 5′ to the mismatch (3) and the demonstration that different exonucleases are required for repair of 3′- and 5′-heteroduplexes (2). The mode of excison during a given repair event is, however, largely unidirectional as judged by action of the system on the circular heteroduplexes used in our experiments. With these circular molecules, it is usually that portion of the unmodified strand spanning the shorter path between the mismatch and d(GATC) sequence that is targeted for excision, and this occurs without regard to polarity of this segment.

A greater degree of variability in location of excision tract end points near the d(GATC) site was observed with the 5′-heteroduplex, as compared with the 3′-substrate, in both cell-free extracts and in the purified system that contained both exonuclease VII and exonuclease I. As judged either by electron microscopy or indirect end-labeling, excision tracts produced on 5′-heteroduplexes often extended into the region 5′ to the d(GATC) sequence. As described above, this effect may be due to abortive attempts of the repair system to excise via the longer path separating the two sites in the circular substrate, or alternatively to nonspecific 3′ → 5′ exonuclease attack on exposed termini that accumulate in repair reactions under conditions of DNA synthesis block. We cannot distinguish between these possibilities.

These experiments have also clarified the mechanism of the excision reaction. We have shown that DNA helicase II is necessary for excision on both 3′- and 5′-heteroduplexes. Thus, like MutH, MutL, MutS, SSB, and DNA polymerase III holoenzyme (1), helicase II is required for repair of both heteroduplex orientations. By contrast, the requirements for exonuclease I and exonuclease VII (or RecJ) are orientation-specific (2). A mechanism for the methyl-directed reaction that incorporates these findings is shown in Fig. 7. The observation that excision on either the 3′- or the 5′-heteroduplex requires cooperation of helicase II and the appropriate exonuclease strongly suggests that excision is strictly exonucleolytic, proceeding from the incision introduced at the d(GATC) site during initiation of repair (3) toward the mismatch. Such a mechanism requires that the repair system to evaluate the orientation of the heteroduplex to ensure that excision from the d(GATC) site proceeds with the proper directionality.

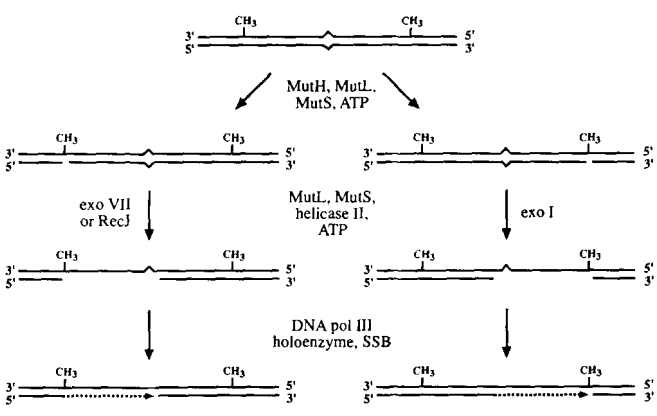

FIG. 7. **Mechanism of methyl-directed mismatch repair.** Repair is initiated by activation of a latent MutH endonuclease in a reaction that is dependent on a mismatch, MutS, MutL, and ATP hydrolysis (3). The activated form of MutH cleaves the unmodified strand at a d(GATC) site that can be located on either side of the mismatch. Excision subsequently removes DNA spanning the two sites, with ensuing repair synthesis initiating near the d(GATC) site or the mismatch, depending on polarity of the unmodified strand. MutS and MutL are shown as required for the excision stage of mismatch correction since they are necessary for repair of preincised heteroduplex (1), perhaps for loading the appropriate excision activities. Involvement of SSB in excision has not been tested.

While methyl-directed mismatch correction shares certain similarities with the reaction catalyzed by the UvrABCD-dependent nucleotide excision repair system, our findings indicate fundamental differences in the modes of action of the two systems. During the course of nucleotide excision repair, the UvrABC excinuclease introduces strand breaks on each side of a lesion, with the intervening oligonucleotide displaced from the helix in a reaction dependent on DNA helicase II (the *uvrD* or *mutU* gene product) and DNA polymerase I (17). Although endonucleolytic cleavage at the d(GATC) site is clearly involved in methyl-directed repair, we have previously discussed our inability to identify occurrence of a second endonucleolytic event near the mismatch (3). The results shown in *lane 5* of Figs. 3 and 4 provide additional evidence for the absence of an endonucleolytic incision near the mispair. If a second incision near the mismatch were to be involved, then these results imply that its occurrence on a 5′-heteroduplex would specifically require exonuclease VII, while the corresponding event on the 3′-substrate would depend on exonuclease I. Since this seems highly unlikely, we favor an excision mechanism in which helicase II displacement renders the incised, unmodified strand sensitive to the appropriate single-strand exonuclease, with hydrolysis commencing at the d(GATC) terminus and proceeding to a point beyond the mismatch.

For both 5′- and 3′-heteroduplexes, excision tracts were found to terminate within the 100-nucleotide region just beyond the mispair in the major subpopulation of product molecules. The mechanism by which excision terminates at this location remains to be defined, but it presumably involves negative or positive modulation of the excision process by other components of the repair system. The component(s) responsible for control of the excision process may act to block helicase or exonuclease action after removal of the mispaired base from the helix or, alternatively, may serve to activate the excision system only so long as a mismatch is present.

Although surprisingly complex, a bidirectional mechanism for strand-specific mismatch repair appears to be highly conserved in nature. The accompanying manuscript (8) describes the nature of the excision reaction associated with the general, strand-specific mismatch repair pathway in human cells. Not only does the human system display a mismatch specificity similar to that of the bacterial reaction (8, 18, 19), but it shares a bidirectional excision mechanism with properties that are essentially identical with those described here for the bacterial pathway.

REFERENCES

1. Lahue, R. S., Au, K. G., and Modrich, P. (1989) *Science* **245**, 160–164
2. Cooper, D. L., Lahue, R. S., and Modrich, P. (1993) *J. Biol. Chem.* **268**, 11823–11829
3. Au, K. G., Welsh, K., and Modrich, P. (1992) *J. Biol. Chem.* **267**, 12142–12148
4. Längle-Rouault, F., Maenhaut-Michel, G., and Radman, M. (1987) *EMBO J.* **6**, 1121–1127
5. Lehman, I. R., and Nussbaum, A. L. (1964) *J. Biol. Chem.* **239**, 2628–2636
6. Chase, J. W., and Richardson, C. C. (1974) *J. Biol. Chem.* **249**, 4553–4561
7. Lovett, S. T., and Kolodner, R. D. (1989) *Proc. Natl. Acad. Sci. U. S. A.* **86**, 2627–2631
8. Fang, W., and Modrich, P. (1993) *J. Biol. Chem.* **268**, 11838–11844
9. Lahue, R. S., Su, S.-S., Welsh, K., and Modrich, P. (1987) in *DNA Replication and Recombination: UCLA Symposium on Molecular and Cellular Biology New Series* (McMacken, R., and Kelly, T. J., eds) Vol.

47, pp. 125–134, Alan R. Liss, Inc., New York
10. Su, S.-S., Lahue, R. S., Au, K. G., and Modrich, P. (1988) *J. Biol. Chem.* **263,** 6829–6835
11. Maniatis, T., Fritsch, E. F., and Sambrook, J. (1982) *Molecular Cloning: A Laboratory Manual,* Cold Spring Harbor Laboratory Press, Cold Spring Harbor, NY
12. Lu, A.-L., Clark, S., and Modrich, P. (1983) *Proc. Natl. Acad. Sci. U. S. A.* **80,** 4639–4643
13. McHenry, C., and Kornberg, A. (1977) *J. Biol. Chem.* **252,** 6478–6484
14. Su, S.-S., Grilley, M., Thresher, R., Griffith, J., and Modrich, P. (1989) *Genome* **31,** 104–111
15. Maxam, A. M., and Gilbert, W. (1980) in *Methods in Enzymology: Nucleic Acids Part I* (Grossman, L., and Moldave, K., eds) Vol. 65, pp. 499–560, Academic Press, NY
16. Church, G. M., and Gilbert, W. (1984) *Proc. Natl. Acad. Sci. U. S. A.* **81,** 1991–1995
17. Sancar, A., and Sancar, G. B. (1988) *Annu. Rev. Biochem.* **57,** 29–67
18. Holmes, J. J., Clark, S., and Modrich, P. (1990) *Proc. Natl. Acad. Sci. U. S. A.* **87,** 5837–5841
19. Thomas, D. C., Roberts, J. D., and Kunkel, T. A. (1991) *J. Biol. Chem.* **266,** 3744–3751
20. Lahue, R. S., Su, S. S., and Modrich, P. (1987) *Proc. Natl. Acad. Sci. U. S. A.* **84,** 1482–1486